ACS APPLIED MATERIALS & INTERFACES

Research Article

www.acsami.org

Transfection System of Amino-Functionalized Calcium Phosphate Nanoparticles: In Vitro Efficacy, Biodegradability, and Immunogenicity Study

Babak Mostaghaci,[†] Julia Susewind,[§] Guido Kickelbick,[‡] Claus-Michael Lehr,*[,†,§] and Brigitta Loretz*[,†]

[†]Department of Drug Delivery (DDEL), Helmholtz-Institute for Pharmaceutical Research Saarland (HIPS), Helmholtz Centre for Infection Research (HZI), Saarland University, 66123 Saarbrücken, Germany

[‡]Inorganic Solid State Chemistry, Saarland University, Am Markt Zeile 3, 66125 Saarbrücken, Germany

[§]Biopharmacy and Pharmaceutical Technology, Department of Pharmacy, Saarland University, Saarbrücken, Germany

Supporting Information

ABSTRACT: Many methods have been developed in order to use calcium phosphate (CaP) for delivering nucleotides into living cells. Surface functionalization of CaP nanoparticles (CaP NPs) with N-(2-aminoethyl)-3-aminopropyltrimethoxysilane was shown recently to achieve dispersed NPs with a positive surface charge, capable of transfection (*Chem. Mater.* **2013**, *25* (18), 3667). In this study, different crystal structures of amino-modified CaP NPs (brushite and hydroxyapatite) were investigated for their interaction in cell culture systems in more detail. Qualitative (confocal laser scanning microscopy) and quantitative (flow cytometry) transfection experiments with two cell lines showed the higher transfection efficacy of brushite versus hydroxyapatite. The transfection also revealed a cell type dependency. HEK293 cells were easier to transfect compared to A549 cells. This result was supported by the cytotoxicity results. A549 cells showed a higher degree of tolerance toward the CaP NPs. Further, the impact of the surface modification on the interaction with macrophages and complement as two important components of the innate immune system were considered. The amine surface functionalization had an effect of decreasing the release of proinflammatory cytokines. The complement interaction investigated by a C3a complement activation assay did show no significant differences between CaP NPs without or with amine modification and overall weak interaction. Finally, the degradation of CaP NPs in biological media was studied with respect to the two crystal structures and at acidic and neutral pH. Both amino-modified CaP NPs disintegrate within days at neutral pH, with a notable faster disintegration of brushite NPs at acidic pH. In summary, the fair transfection capability of this amino functionalized CaP NPs together with the excellent biocompatibility, biodegradability, and low immunogenicity make them interesting candidates for further evaluation.

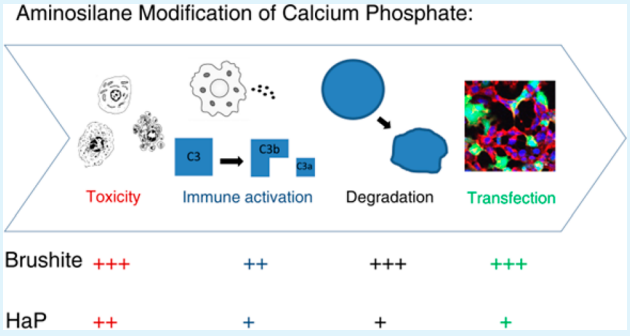

KEYWORDS: *aminosilane, biodegradation, gene delivery, nucleotides, complement activation, cytokine release*

1. INTRODUCTION

Gene therapy is a modern therapeutic paradigm in which the number of related clinical trials and targeted diseases is slightly increasing.[1] Especially in recent years, the need of having suitable nucleotide delivery system is stimulated by the current advancements in genome editing tools such as zinc-finger nuclease (ZFNs), transcription activator-like effector nucleases (TALENs), and (CRISPR)/Cas-based methods.[2,3] The vast majority of clinical trials in gene delivery was conducted with viral vectors.[1] Despite that fact, gene delivery with nonviral carriers was progressively investigated because of the safety concerns that appeared with viral vectors on the host immune tolerance and the possibility of generating replication-competent viruses.[4,5] Many types of nonviral vectors such as dendrimers,[6] polypeptides,[7,8] lipids,[9] polysaccharides,[10] cationic polymers,[11] and particles of varying composition[12−14] have been studied for their toxicity and transfection efficiency. Furthermore, inorganic nanoparticles (NPs) such as gold,[15] iron oxide,[16] silica,[17−19] and layered double hydroxide[20] were used for gene delivery applications because of their simple synthesis and administration and lower toxicity in comparison to polymeric materials.[21] Calcium phosphate (CaP) has almost a four-decade history regarding in vitro gene delivery.[22] The capability for interaction with nucleotides and the good biocompatibility has made this material a proper choice for gene delivery. In contrast, their poor transfection efficiency, and the high dependency of their colloidal properties on the process parameters during synthesis hinder their further applications in nonviral gene delivery area. Major issues are the colloid agglomeration of the particles resulting in their instability and

Received: October 17, 2014
Accepted: February 18, 2015
Published: February 18, 2015

DOI: 10.1021/am507193a
ACS Appl. Mater. Interfaces 2015, 7, 5124−5133

missing storage stability. Hence, there have been always some efforts to improve their properties.[23,24]

Addition of polymeric substances to CaP,[25] coating with lipids,[26] preparing multishell calcium phosphate-pDNA,[27] and PEGylation[28] are some of the examples for improving the transfection efficiency. However, the problems regarding the agglomeration of the particles, instability of NPs dispersion, and low transfection efficiency remain in most of the improved systems.

We recently reported a new method for in situ synthesis and functionalization of CaP NPs with an aminosilane (N-(2-aminoethyl)-3-aminopropyltrimethoxysilane, APTMS) for gene delivery applications.[29] Some preliminary biological experiments revealed that these particles, having positive surface charge, were capable of transfecting A549 cells. We showed that the presence of APTMS has an effect on the crystal structure of produced CaP. At pH 5, brushite was produced with or without the presence of APTMS. At pH 7 without APTMS, brushite was obtained, whereas with the addition of APTMS, hydroxyapatite (HaP) was formed. The assumption was that this behavior happens because of oriented nucleation and growth of CaP crystallites that were proven by microstructural analysis on X-ray diffraction data.

The motivation for this study was to understand if the differences in surface modification have an impact on the various interactions with biological tissue. Thus, we studied not only the transfection and cytotoxicity in more detail but also analyzed the interaction with the immune system. Cytokine release by macrophages and complement activation were chosen here as important components of the innate immune response. If the amine-functionalization helps or at least not worsen the inertness toward the immune system, this could be an interesting way to stabilize particles. Of further importance for a planned in vivo application is also the biodegradation behavior of the carrier. The two different crystal structures were thought to result in different dissolution behavior. A fast degradation and elimination should be a favorable property for a carrier of nucleotide actives with transient action.

2. EXPERIMENTAL SECTION

2.1. Materials. The reagents needed for preparing the particles, diammonium hydrogen phosphate ($(NH_4)_2HPO_4$, phosphate solution), calcium nitrate tetrahydrate ($Ca(NO_3)_2{\cdot}4H_2O$, Ca solution), *N*-(2-aminoethyl)-3-aminopropyltrimethoxysilane (APTMS), glacial acetic acid, and ammonium hydroxide (NH_4OH) solution, were obtained from Merck (Darmstadt, Germany). Ultra purified water that was used in all parts of this research was prepared using Milli-Q system (Merck Millipore, Billerica, USA). For cytotoxicity test, an LDH kit was purchased from Roche Applied Science (Penzberg, Germany). Luciferase assay kit was purchased from Promega (Fitchburg, USA). pAmCyan (encoding a cyan fluorescent protein) and pGL3 (a luciferase reporter vector) plasmids were received from Clontech (Mountain View, CA, USA) and Promega, respectively. Qiagen EndoFree Plasmid Mega Kit (Qiagen, Hildesheim, Germany) was used to isolate both plasmids after propagation in *E. coli* DH5α. A549 (CCL-185) and HEK293 (CRL01573) cells were obtained from ATCC (Manassas, VA, USA). Dulbecco's modified Eagle's medium (DMEM) was used to cultivate both cell lines that was received from GIBCO (Karlsruhe, Germany). The fresh human blood used for blood compatibility was a kind donation from Klinikum Saarbrücken (Winterberg, Saarbrücken, Germany). The isotonic phosphate buffer for washing and suspending the erythrocytes was prepared as follows: 6.78 g of NaCl, 1.42 g of Na_2HPO_4 and 0.4 g of KH_2PO_4 were dissolved in 1 L of purified water, adjusting the pH at 7.4 and the osmolarity on 300 mOsmol/L. For the measurement of cytokine release CBA Flex Sets for IL-8, IL-6, IL-1ß, and TNFα were obtained from BD Biosciences (Heidelberg, Germany). THP-1 cells were purchased from the DSMZ (Deutsche Sammlung von Mikroorganismen und Zellkulturen, Braunschweig, Germany). RPMI1640 cell culture medium was obtained from Gibco (Carlsbad, CA) and FBS from PAA (Pasching, Austria). Phorbol myristate acetacte (PMA) was obtained from Sigma (München, Germany). For C3a complement activation assay, MicroVue C3a Plus EIA Kit, normal human serum complement (NHS, C3a concentration: 886 ng/mL) and cobra venom factor (CVF, as positive control, 680 units/mL) were obtained from Quidel (San Diego, CA, USA). Polyethylenimine (PEI, M_W 25 kDa, Sigma-Aldrich, MO, USA), poly(D,L-lactide-*co*-glycolide) (PLGA, RESOMER RG 752H 75:25, Evonik, Essen, Germany), and poly(vinyl alcohol) (PVA, Kuraray Europe, Hattersheim am Main, Germany) were used to prepare PEI/pDNA[30] and PVA-stabilized PLGA NPs[31] as benchmarks in immunological experiments. As a benchmark for transfection, a commercial transfection reagent called jetPRIME (polyplus, Illkirch, France) was used.

2.2. Synthesis of Nanoparticles and Characterization. The detailed methods for synthesis and characterization of the pristine and amino-modified CaP NPs (amCaP) were described previously.[29] Briefly, APTMS was added to 10 mL of pH adjusted 0.1 M phosphate solution. After stirring for 15 min, 20 mL of pH adjusted 0.1 M Ca solution was added this mixture. Glacial acetic acid was used for adjusting the pH on 5 or 7. After 4 h of stirring at room temperature, the particles were washed using a dialysis membrane (MWCO: 12−14 kDa, Thermofischer, Waltham, USA). The dialysis was performed against 10 L of purified water and the washed particles were freeze-dried (Alpha 2−4 LSC lyophilizer, Christ, Osterode, Germany) afterward for storage. The same route without adding APTMS was used in the synthesis of pristine CaP particles.

All the prepared particles were characterized using dynamic light scattering (DLS) and transmission electron microscopy (TEM) regarding morphology and surface charge. X-ray diffraction (XRD) was used for investigating their crystal structure and CHN elemental analysis and TNBS colorimetric experiment to determine their surface chemistry.

To analyze the completeness of DNA binding, we performed a gel retardation assay, which is a standard method for this purpose.[32] Complexes of amCaP NPs and pDNA with the weight ratios of particles to pDNA ranging from 0.5 to 100 were prepared and incubated for 30 min at 37 °C. Gel electrophoresis was conducted in 1% agarose gel, 0.5× TBE buffer, at 50 V for 2 h. Ethidium bromide was added to the agarose gel as staining agent. Molecular imaging system FusionFX7 (Peqlab Biotechnology, Erlangen, Germany) was used to study the amount of free and bound pDNA.

2.3. Degradation in Biorelevant Media. For investigating the disintegration of the amCaP NPs over time, we measured the release of Ca^{2+} and Si^{4+} ions. An ICP-OES (Inductive Coupled Plasma−Optic Emission-Spectrometry, Optima 2000 DV, PerkinElmer, USA) was used for ion detection. The NP suspensions were kept in Slide-A-Lyzer dialysis cassettes G2 (Thermo Scientific, Waltham, MA, USA, MWCO: 2 kDa) in order to avoid the interfering of NPs in ions detection procedure. The dialysis cassettes were incubated in 1 L of 0.1 M acetate (pH 4, to simulate lysosome pH) and 0.1 M HEPES (pH 7.4, to simulate blood pH) buffers at 37 °C. The samples were collected at different time steps (for 7 days). Collected samples were repurified by centrifugation using Macrosep advanced centrifugal devices (Pall corp., Port Washington, NY, USA, MWCO: 3 kDa) and stabilized afterward by adding concentrated nitric acid. At the end of the experiment, the remaining particles in the dialysis cassettes were centrifuged and weighed. In an attempt to confirm the results, we analyzed the suspended NPs also using DLS and nanoparticle tracking analysis (NTA) over the experimental period. The measurement allows investigating the alteration in the size, PDI, and concentration of the particles.

2.4. Transfection Efficiency. Analysis of the transfection efficiency was performed on A549 and HEK293 cells using luciferase transfection assay, confocal laser scanning microscopy (CLSM) and flow cytometry. For the transfection, we seeded A549 and HEK293 in

DOI: 10.1021/am507193a
ACS Appl. Mater. Interfaces 2015, 7, 5124−5133

24-well plate with the density of 2.5 × 10^4 cells/well and 1 × 10^4, respectively. Both cell lines were maintained for 48 h to reach 90% confluence. After being washed, the cells were incubated with different concentrations of the NPs carrying pDNA for 4 h and after replacing the NPs suspension with fresh medium the cells went under another incubation procedure for 24 h. pGL3 plasmid DNA (encoding a luciferin protein) was used for luciferase transfection assay and pAmCyan pDNA (encoding a fluorescent protein) was used for CLSM and flow cytometry analysis. Naked plasmid DNA was used as a negative control and JetPrime, a commercial transfection reagent, was added as a positive control. In luciferase assay, conventional CaP transfection reagent (CalPhos, Clontech, USA) was used as a second positive control in the optimum concentration recommended by the manufacturer. The amount of pDNA in all of the wells was kept constant on 1 μg.

For the luciferase transfection assay, the cells were lysed after incubation and the luminescent intensity was measured after adding luciferase assay reagent using Tecan microplate reader. For CLSM observation, we stained the transfected cells using DAPI (emission, 461 nm; excitation, 374 nm) as cell nuclei staining and RRCA (emission, 550 nm; excitation, 575 nm) to stain the cell membrane. The cells were studied using Zeiss LSM 510 Meta confocal microscope (Göttingen, Germany) and analyzed by means of Zeiss LSM 510 software. DAPI (excitation, 360 nm; band-pass filter, 390−465 nm), rhodamine (excitation, 488 nm; band-pass filter, 500−530 nm), and AmCyan (excitation, 543 nm; band-pass filter, 560−615 nm) channels were used for capturing of images that were taken using 63× water immersion objective.

For flow cytometer analysis, the cells were washed 3 times and detached from the wells by applying trypsin enzyme and incubating them for 5 min at 37 °C. After centrifugation at 1000g for 5 min the cell pellet was suspended in 500 μL of cell culture medium. The percentage of transfected cells were measured by means of BD FACSCalibur (Becton-Dickinson, Heidelberg, Germany) and analyzed using FlowJo software FlowJo (version 7.2.5, Tree Star, Stanford, CA, USA). 10000 cells were analyzed for each sample. For the excitation, an argon laser with a wavelength of 488 nm was used, and emission was recorded through a 515−545 nm filter.

2.5. Cytotoxicity and Blood Compatibility. To evaluate the cytotoxicity of the amCaP NPs, we conducted LDH and MTT assays over a broad range of concentrations (0.05−10 mg/mL). For this purpose, A549 and HEK293 were seeded in 96-wells plate with the density of 1000 cells/well 48 h before the cytotoxicity experiments to reach 90% confluence. The cells were washed using PBS buffer and incubated for 4 h with different concentration of the particles dispersed in DMEM medium at 37 °C. Pure DMEM medium and 1% Triton X-100 were used as positive and negative controls, respectively. The supernatant was separated afterward and after mixing with LDH substrate and 5 min of incubation its absorbance was read at 492 nm using Tecan Infinite 200 microplate reader. The cells were washed and incubated with MTT reagent ((3-(4,5-dimethylthiazol-2-yl)-2,5-diphenyltetrazolium bromide) for another 4 h and dissolved using DMSO afterward. The amount of released formazan content, as an index for metabolic activity of the cells, was determined by measuring the absorbance at 550 nm using a microplate reader. The viability of the cells was calculated by considering the absorbance of positive and negative control as 100% and 0% cellular viability, respectively. The LC_{50} diagram was plotted using dose−response curve fitting (OriginPro, Ver 8.6.0, OriginLab Corp., USA). The graph enables us to estimate the critical particle concentrations that kill 20 and 50% of the cells.

For the blood compatibility assay, fresh erythrocytes were isolated from the blood of healthy donors. The erythrocytes were separated via a centrifugation at 12000g for 10 min, and washed with the isotonic phosphate buffer three times. The final erythrocytes suspension in the buffer had a concentration of 2% v/v. 200 μL of each sample (adjusted to 300 mOsmol with NaCl) was added to 500 μL of erythrocyte suspension in 24-well plate, and the plate was incubated at 37 °C for 3 h. After centrifugation at 1500g for 5 min the absorbance of the samples at 540 nm was measured using Tecan microplate reader. The percentage of hemolysis was calculated by comparing the results with the absorbance of negative (2% Triton X-100) and positive (Buffer) controls.

2.6. Immunological Investigations. For investigating the immunological response toward the unmodified and modified NPs, we studied the effect of NPs on macrophage cytokine secretion and C3a complement activation.

Measurement of cytokine release (IL-8, IL-6, IL-1ß, and TNFα) was carried out by flow cytometer (FACSCalibur, BD Biosciences) and analysis was performed via FCAP array v3.0.1 cytometric bead array analysis software. For this purpose, THP-1 cells differentiated to macrophage-like cells were used. The human monocytic cell line THP-1 was cultured in T75 cell culture flasks with RPMI1640 supplemented with 10% FBS at 37 °C and 5% CO_2. To differentiate THP-1 in macrophage-like cells, 5 ng/mL PMA was added to the cell culture medium. After 48 h, cells were used for the experiment. Cells were seeded in a 24 well plate and were incubated with 0.5, 0.1, and 0.05 μg/mL of the different nanoparticles. After 24 h incubation, 50 μL of cell supernatant was collected and prepared for the analysis following the manufacturer protocol. Cell culture medium was used as a negative control and LPS as a positive control.

C3a complement activation assay was conducted with reference to the guideline provided by the manufacturer. Briefly, 100 μL aliquots of normal human serum (NHS) were incubated with two concentrations of unmodified and modified particles (0.05 and 0.5 mg/mL) for 30 min at 37 °C. As positive control, 10 μL of EDTA (220 mM) was added to NHS (to inhibit to activation of C3a), and as negative control, 3 μL of cobra venom factor (CVF) was added (that supposed to activate the whole C3a). The reaction was stopped by adding 10 μL of EDTA (220 mM) to each sample. After diluting the samples 5000 times, 100 μL were added to the 96-well ELISA plate (coated with a murine monoclonal antibody) and incubated for 1 h at room temperature. The wells were washed 4 times afterward, and 100 μL of conjugate (contains horseradish peroxidase-conjugated polyclonal antibody to C3a) was added. The ELISA plate was incubated at room temperature for another 1 h and washed afterward, and then 100 μL of substrate solution (containing 3,3′,5,5′-tetramethylbenzidine and H_2O_2) was added to each well. After incubating at room temperature for 15 min in darkness, 100 μL stop solution (1 N HCl) was added to each well, and the absorption at 450 nm was read using a microplate reader. A calibration curve based on the absorption of solutions with standard C3a concentration (provided by the manufacturer) was plotted using a 4-parameter curve fit and used to determine the concentration of the samples. Cobra venom factor was used as positive control and EDTA inhibited NHS was used as a negative control. The results were normalized considering the positive control as 0 ng/mL C3a. In both immunological experiments, PEI/pDNA and PVA-stabilized PLGA NPs were investigated as benchmarks.

3. RESULTS AND DISCUSSION

3.1. Physicochemical Specifications. It was previously reported that brushite and HaP NPs were prepared based on the pH in the synthesis procedure. Brushite NPs had a hydrodynamic size of 139.1 ± 15.4 nm with a positive surface charge of 13.8 ± 0.6 mV at physiological pH. The hydrodynamic size and zeta potential of HaP NPs at physiological pH were 145 ± 19.8 nm and 4.5 ± 0.7 mV, respectively. The higher surface charge of brushite NPs in comparison to HaP NPs was related to the amine density on the surface of NPs. By means of TNBS colorimetric experiment, it was revealed that the amount of amine groups on the surface of brushite and HaP NPs was 15.1 ± 0.6 m^2 g^{-1} and 3.2 ± 0.4 m^2 g^{-1}, respectively. Using these values and the specific surface area of the particles obtained from BET experiment, we calculated the amine density of the NPs. The surface area was much higher in the case of brushite NPs (25.9 ± 3.1 μmolm^{-2}) than HaP NPs (3.42 ± 0.5 μmolm^{-2}). Both

DOI: 10.1021/am507193a
ACS Appl. Mater. Interfaces 2015, 7, 5124−5133

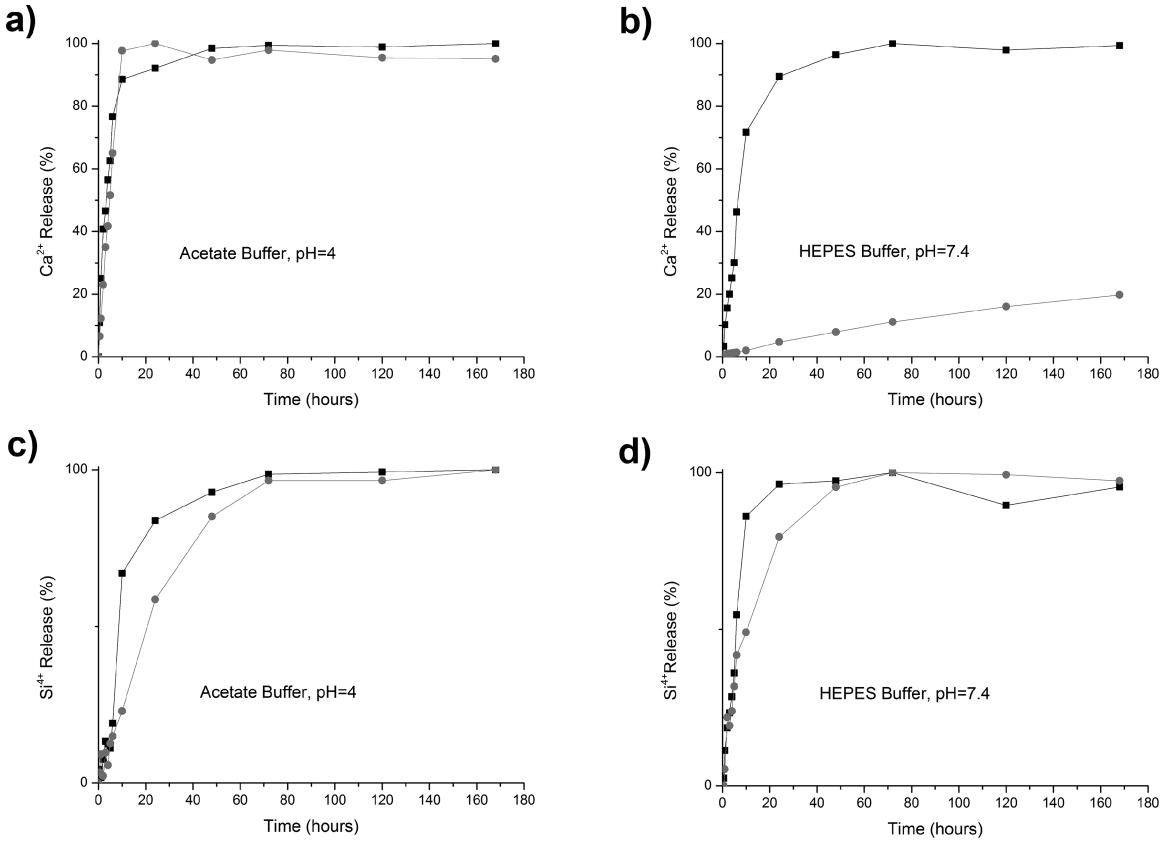

Figure 1. Release of Ca^{2+} and Si^{4+} ions from brushite and HaP NPs in (a, c) acetate buffer with pH 4 and (b, d) HEPES buffer with pH 7.4; ■, brushite, and ●, HaP NPs.

types of NPs showed a narrow-size distribution.[29] A gel retardation assay showed the capability of both modified NPs to condense pDNA (see the Supporting Information, Figure S1). For brushite and HaP NPs, the complete condensation of pDNA was obtained at NPs/pDNA weight ratio of 40 and 50, respectively.

3.2. Degradation of the NPs in Biorelevant Media. To see the disintegration behavior of modified CaP NPs at acidic and neutral pH, the release of Ca^{2+} and Si^{4+} ions after suspending the NPs in according buffers were measured. The selected pHs are important regarding the fate of the particles in actual living system. pH 7.4 is the physiological pH of the blood, so it can simulate the general body environment. It becomes more important when we take this fact into account that lacking the biodegradation behavior is a major drawback regarding the biocompatibility of the NPs intended to use for drug delivery purposes.[33] On the other hand when CaP NPs are expected to use in gene delivery studies their solubility in endosome/lysosome conditions become also important. It was shown before that partial dissolution of CaP can facilitate the release of NPs/pDNA into the cytoplasm by destabilization of lysosomal membrane leads to increase the gene delivery efficiency.[34] Hence, we studied the solubility of the NPs at pH 4 to mimic the conditions pertain to the lysosome.

Figure 1 depicts the percentage of ions released in relation to the initial ion content of the particles in order to facilitate the comparison of the disintegration extent. It was revealed that both particles (brushite and HaP) are completely soluble at pH 4 (Figure 1a), as no remaining was found in the dialysis cassette after the experiment. At pH 7.4, we had different dissolution behaviors (Figure 1b). In this case, brushite particles dissolved completely again, but the dissolution rate is not as high as the case of pH 4 and it remained stable for the first few hours. This finding is in agreement with the stability studies that we performed on the particles in our previous work.[29] However, the solubility of HaP NPs is much lower at pH 7.4 in comparison to pH 4 as expected regarding literature.[35] It is possible to see that only a small part of HaP NPs degraded within 7 days. These results were confirmed by weighting the remaining particles in the cassette. As mentioned before in the case of acetate buffer, there was not any remaining for both particles, but in the case of HEPES buffer, 1.51 mg of brushite and 8.39 mg of HaP NPs were found. To have a better understanding, another version of the ions release diagrams based on absolute values of Ca^{2+} and Si^{4+} ions (and not the ions percentage) is presented in the Supporting Information (Figure S2). The higher absolute amount of calcium release from HaP NPs in comparison to brushite NPs is because of the different Ca/P ratios (1 for brushite and 1.67 for HaP)

These results were followed by measuring the release of Si^{4+} ions from the particles at pH 4 and 7.4 to investigate the degradation of the aminosilane coating (Figures 1c and 1d). At both pH, the aminosilane coating degraded completely. At pH 4 (Figure 1c) the Si^{4+} ions release rate was lower than the release rate of Ca^{2+} ions. This is because of the time that is needed for hydrolysis of siloxane bond and release of Si^{4+} ions and is not dependent on the degradation of CaP particles. At pH 7.4 (in Figure 1d), the same behavior was observed, but at this pH the release of Si^{4+} ions were faster than at pH 4. The causative reason is the hydrolytic degradation rate of aminosilane coating is increasing with increasing pH.[36]

DOI: 10.1021/am507193a
ACS Appl. Mater. Interfaces 2015, 7, 5124−5133

We confirmed these results by investigating the size, PDI, and concentration of the suspended particles (at pH 7.4) by means of DLS and NTA methods (Figure S3 and Table S1 in the Supporting Information). Dynamic light scattering methods are not suitable to investigate the degradation of the particles, while two mechanisms of degradation and agglomeration of the particles were continuing at the same time. Moreover, because of the agglomeration of the NPs, the PDI values increased over time that made the measurements unreliable. However, the only reliable measured changes were an increase in the PDI and the weaker fit with the autocorrelation function that can be seen for both brushite and HaP NPs within the 48 h of incubation time. On the other hand, the concentration of the particles resulted from NTA method showed a decreasing in the number of the NPs. This is more important when we consider this fact that we sonicated the particles and filtered them (0.45 μm) before NTA analysis, so this reduction could be because of the degradation of the particles.

Figure 1c, d shows the amount of silicon ion release over time at different pH. It was revealed that at both pH 4 and 7.4 and for both brushite and HaP, the entire silane coating degraded. The higher silicon release rate in the case of brushite in comparison to HaP NPs is related to the higher solubility of these particles that form the core part of NPs. Even at pH 7.4, although the entire HaP did not solubilize, but the silane coating completely degraded. This is in agreement with the literature regarding the degradation of silane coating in the presence of water at the temperature around 40 °C because of siloxane bond hydrolysis.[37] The difference in the Si^{4+} release between brushite and HaP NPs can be explained by the higher density of aminosilane modification as mentioned in section 3.1.

3.3. Transfection Experiments. Our primary luciferase experiments on modified brushite and HaP NPs already showed that both NPs were capable of transfecting A549 cells over a broad range of particle concentration. We selected the concentrations that led to highest transfection efficiency and transfected the cells with a fluorescent protein encoding pDNA (pAmCyan). We reached quite promising results using confocal laser scanning microscopy, as it was possible to see the transfection capability of the NPs.[29] In this study, the aim was to prove the potency of NPs as nonviral gene delivery carriers by transfection of HEK293 cells using brushite and HaP NPs. HEK293 cells are epithelial adherent cells and often used as a host in transfection models.

Figure 2 shows the results of luciferase transfection assay. It was revealed that both NPs were capable to transfect HEK293 cells over a broad range of concentration but as expected using brushite NPs resulted in higher transfection efficiency because of the higher density of amine groups on their surface. Brushite NPs displayed their maximum transfection efficiency in lower particles to pDNA weight ratios in comparison to HaP NPs. Overall, the transfection results of HEK293 are in accordance with the A549 transfection results. Brushite NPs was superior in both cell lines.

Conventional CaP showed low transfection efficiency in comparison with modified brushite and HaP NPs. The transfection results with this reagent varied in a broad range in the different times of the experiment, demonstrating a lack of reproducibility.

The results from luciferase transfection assay was confirmed using confocal laser scanning microscopy (Figure 3). Figure 3a shows HEK293 cells after adding naked pAmCyan pDNA.

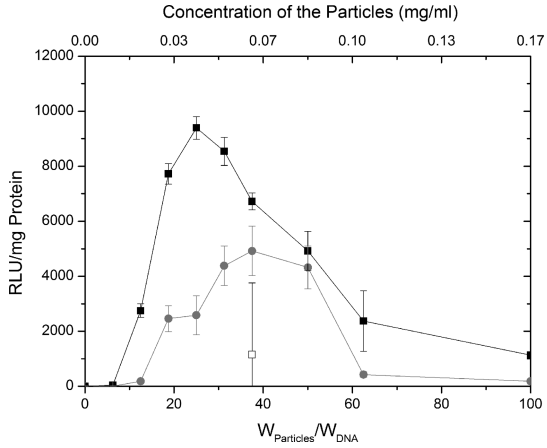

Figure 2. Results of luciferase transfection assay after transfecting HEK293 cells with pGl3 pDNA using ■, brushite; and ●, HaP NPs. Conventional CaP transfection reagent (□) was used as positive controls for transfection in the optimum concentrations recommended by the manufacturer.

Even if some transfection happened, it was not significant to trace it using the fluorescent effect emitted from the translated protein. Using brushite and HaP NPs (Figure 3a, b) resulted in considerable transfection of the cells but as a qualitative proof for the luciferase assay, it can be seen that brushite NPs led to more efficient transfection in comparison to HaP NPs. Figure 3d shows the HEK293 cells after transfecting using the commercial transfection reagent (JetPrime). The cells seem to be more transfected with the fluorescent protein in comparison to the samples that were transfected with CaP NPs. However, we already showed that JetPrime has some toxic effects on A549 cells as the morphology of the cells changed after adding this reagent.[29] In the case of HEK293 cells, this phenomenon could not be seen.

The percentage of transfected A549 and HEK293 cells after transfecting them with pAmCyan pDNA were measured using flow cytometer analysis (Figure 4). As expected from the luciferase transfection assay and CLSM analysis, brushite NPs led to transfect of the larger number of cells in comparison to HaP NPs. However, it was revealed that in the case of HEK293 cells, the number of transfected cells is higher than the number of transfected A549 cells. This difference in transfection of A549 and HEK293 cells was seen before using other transfection agents.[38] As a positive control, the transfection efficiency of a commercial transfection reagent (JetPrime) was evaluated using a luciferase assay and flow cytometry. From the flow cytometry results in the case of HEK293 cells, it could be realized that the number of cells transfected with brushite NPs (around 25% in the optimum NPs/pDNA weight ratio) was near to the number of cells transfected by JetPrime (around 33%). Considering the luciferase assay results, however, showed that the amount of transgene expression per cell was higher in the case of JetPrime (18 000 RLU/mg protein for JetPrime in front of 85 000 RLU/mg protein for brushite NPs in the optimum NPs/pDNA weight ratio). These results are in correlation with the CLSM images (Figure 3). Also, here it is visible that brushite NPs and JetPrime resulted in a similar number of transfected cells but in the case of JetPrime the cells showed a higher intensity of green fluorescence. Summing up, the results of transfection experiments showed that brushite

DOI: 10.1021/am507193a
ACS Appl. Mater. Interfaces 2015, 7, 5124−5133

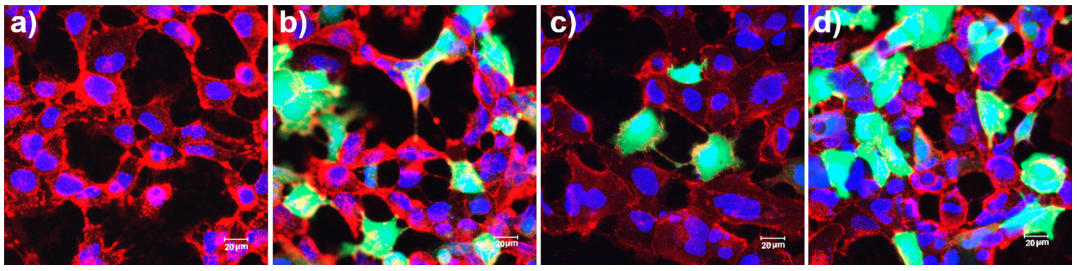

Figure 3. CLSM images of HEK293 after transfecting with pAmCyan pDNA using (a) naked pDNA, as a negative control, (b) brushite NPs, (c) HaP NPs, and (d) jetPrime as commercial transfection agent. Green, fluorescent protein; red, cell membrane; blue, cell nuclei.

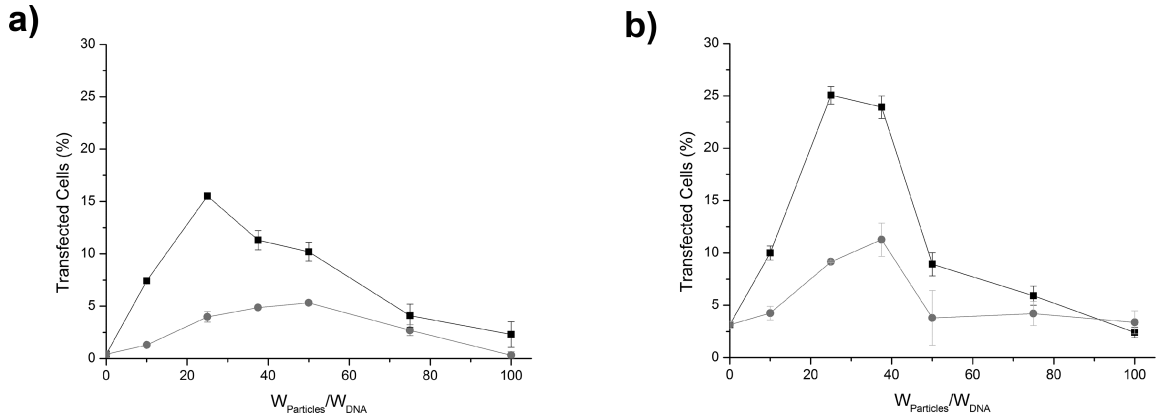

Figure 4. FACS analysis results for (a) A549 and (b) HEK293 cells after transfecting with pAmCyan pDNA using ■, brushite; and ●, HaP NPs.

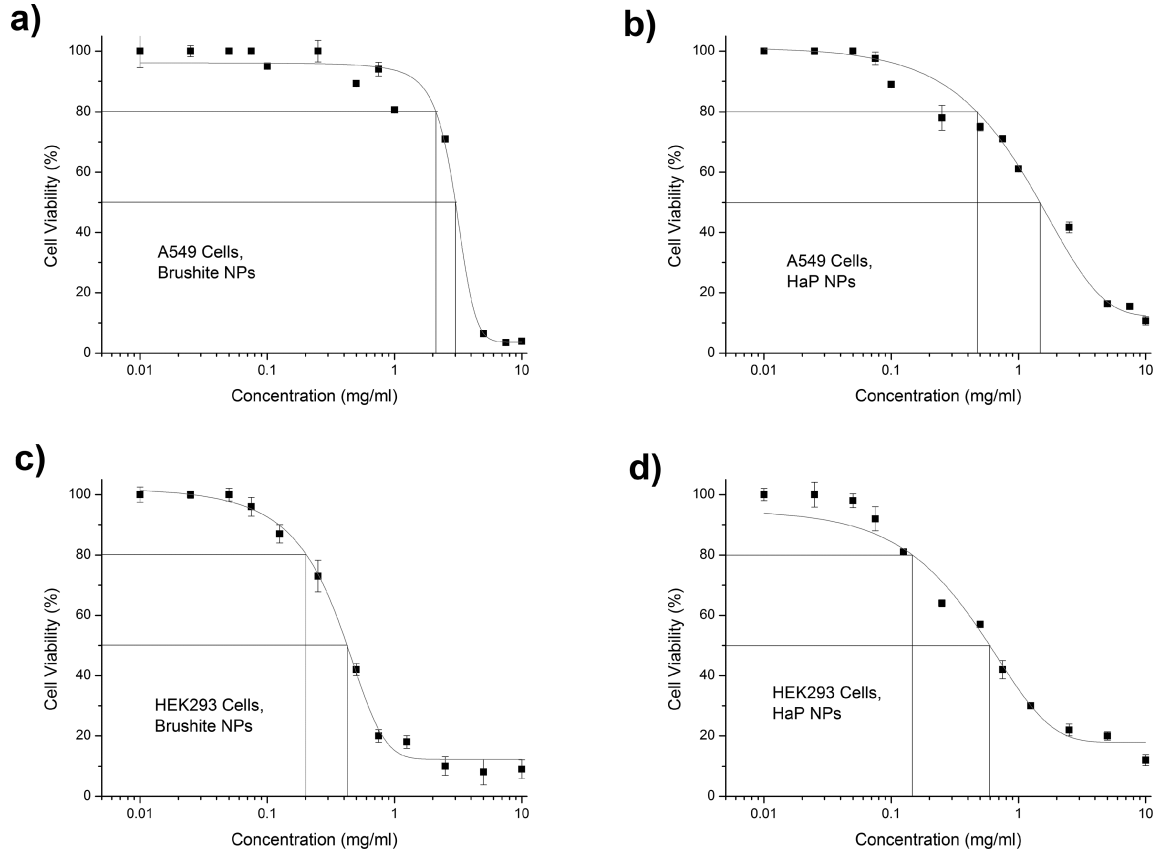

Figure 5. Results of MTT cytotoxicity assay for (a) brushite and (b) HaP NPs incubated with A549 cells and (c) brushite and (d) HaP NPs incubated with HEK293 cells.

DOI: 10.1021/am507193a
ACS Appl. Mater. Interfaces 2015, 7, 5124−5133

and HaP NPs can be used to transfect different cell lines, but brushite NPs resulted in a more successful transfection.

3.4. Cytotoxicity of the NPs. Lactate dehydrogenase (LDH) cytotoxicity assays on A549 and HEK293 showed that there was not any significant cell membrane damage happened in a result of using brushite and HaP NPs (see the Supporting Information, Figure S4). In both cell lines and with both types of NPs the viability of cells was more than 80% up to a concentration of 5 mg NP/mL. As LDH assay only shows the cell membrane damage, we performed an MTT test to investigate the toxicity of the particles monitored by the metabolic activity of the cells. Figure 5 depicts the results of the MTT assay and the calculation of the LC_{50} and LC_{80} values for both types of modified NPs incubated with A549 and HEK293 cells. In the case of A549 cells, the modified brushite particles showed less cytotoxicity in comparison with modified HaP particles. The critical concentrations of brushite particles that killed 20 and 50% of the cells were 2.11 and 3.00 mg/mL, respectively. The LC_{80} and LC_{50} concentrations were 0.47 and 1.478 mg/mL for modified HaP (Figure 2a, b).

For both particles, these concentrations were higher than the concentrations that were required for optimal transfection of A549 cells with pDNA (Section 3.3). The LC_{80} is defined as the concentration of particles that kill 20% of the cells. If we consider LC_{80} as statistical significant toxicity, the LC_{80} concentration was 75 times more than the concentration needed for the optimal transfection for brushite particles. Moreover, in the case of HaP particles the LC_{80} concentration was still 25 times higher than the optimal transfection concentration. So one can consider both particles as comparable low-toxic regarding transfection of A549 cells. In the case of HEK293, the particles show more toxicity toward cells. For brushite NPs, the critical concentrations of the particles that killed 20 and 50% of the cells are 0.20 and 0.42 mg/mL, respectively. In the case of HaP NPs these concentrations were 0.14 and 0.59 mg/mL. However, for both types of NPs, these concentrations were higher than the concentrations that were needed for optimal transfection of HEK293 cells.

For both cell lines, HaP NPs caused a higher cytotoxicity in comparison to brushite NPs. It was mentioned in section 3.1 that the surface charge of brushite NPs was higher than the surface charge of HaP NPs. Surface charge of the particles can lead to their colloidal stability because of electrostatic charge repulsion. From this point of view, it is possible to see that the lower stability of HaP NPs (in comparison with brushite NPs) could lead to partial precipitation of these particles (because of their aggregation), which led to an increased local concentration and the direct contact with the cells. This issue changed the biological environment of the cells and interfered with their viability.

To exemplify the wide gap between the concentration used for transfection and toxic concentrations (e.g., LC_{50} and LC_{80}) CaP NPs were compared against PEI (M_w 25 kDa, branched). The most effective concentration of PEI, which is still a benchmark transfection carrier and is used usually for transfection, is 5 μg/mL. The concentrations of PEI that lead to the death of 50% of the cells are 12 μg/mL in the case of A549 and 9 μg/mL in the case of HEK293 cells.[39,40] The therapeutic window for CaP particles and especially for brushite particles is thus much wider (Supporting Information, Table S2).

3.5. Blood Compatibility of the NPs. Figure 6 shows the results of erythrocytes lysis assay for modified brushite and HaP

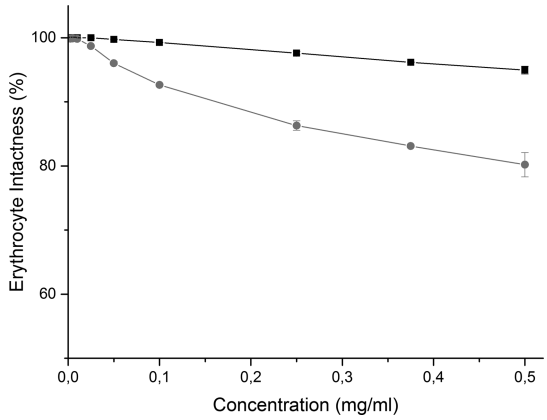

Figure 6. Results of erythrocyte lysis assay for ■, brushite; and ●, HaP NPs.

NPs. When one compares these results to other materials used for gene delivery (e.g., silica NPs[41] and PEI[42]), it can be seen that there were negligible adverse effects of both types of CaP NPs toward the erythrocytes. This is in particularly true for the concentrations that obtained the best results in the transfection experiments (Section 3.3). When we compared brushite and HaP NPs for their ability to destabilize erythrocytes' membrane, we noticed that brushite NPs were more compatible in this manner. We believe that this phenomenon is due to the presence of a higher density of amine groups on the surface as reported previously by other researchers.[43] This can also explain why the LDH assay (that monitors the membrane toxicity) did not show noticeable cytotoxicity for the NPs, whereas the MTT assay revealed a concentration-dependent cytotoxicity for both types of NPs.

3.6. Immune Activation Properties of the NPs. Figure 7 shows the results of the measurement of cytokine (IL-1ß, IL-6, IL-8 and TNFα) release from THP-1 macrophages after 24 h incubation with different concentrations (0.05, 0.1, and 0.5 mg/mL) of modified and unmodified brushite and HaP NPs. The measured cytokines are important inflammatory markers and are expressed by different cell types, but especially by macrophages. They play an important role in the regulation of the immune response, inflammatory reactions, and phagocytosis. IL-8 is a chemo-attractant with some specificity for neutrophils.[44]

In contrast, IL-6 is involved in acute phase response and related to endothelial cell dysfunction and fibrogenesis. IL-1ß and TNF-α are pro-inflammatory mediators that act on many cells of the immune system.[45] Especially for IL-8, there is a high release, but no release from IL-6 could be measured. Nearly all samples incubated with higher NP concentrations show higher cytokine release. After incubation with the modified NPs, a much lower cytokine release could be detected in comparison to the results after incubation with unmodified NPs. One reason for that could be that hydrophilic surfaces seem to provide significant inhibition of macrophage fusion that can result in reduced cytokine release and attenuated inflammatory reactions.[46] Another study showed that different amine termination on NP surfaces can produce different effects on induction of inflammatory cytokines.[47] The other reason could be the lower stability of nonmodified CaP NPs in comparison

DOI: 10.1021/am507193a
ACS Appl. Mater. Interfaces 2015, 7, 5124−5133

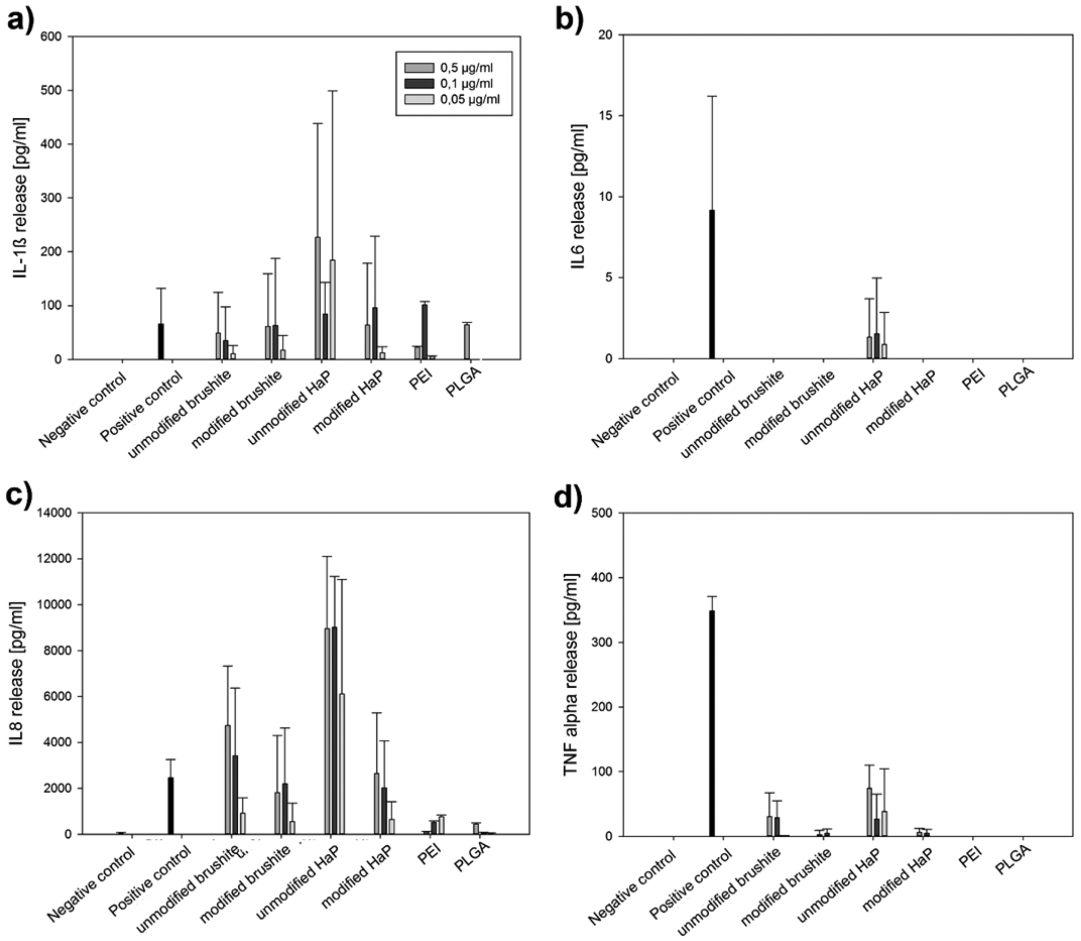

Figure 7. Results of cytokine measurement with THP-1 macrophages after incubation with brushite and HaP NPs. Release of different cytokines was investigated: (a) IL-1β, (b) IL6, (c) IL8, and (d) TNF-α. PEI particles and PLGA particles serve as benchmark particulate references.

to modified CaP NPs that led to their precipitation on the cells. Thus, the increased exposure of the cells to the particles resulted in a more intense stimulation of macrophages and a higher secretion of cytokines.

The comparison between the effect of modified CaP samples and the benchmark NPs (PEI/pDNA & PLGA) on the cytokine release from macrophages showed that the both group have an effect in the same order of magnitude. It can be estimated that amino-modified CaP NPs will not stimulate inflammatory responses considerably more than other well-known NPs used in drug/gene delivery.

The C3a complement activation assay was performed in order to understand the CaP particles vulnerability to complement activated clearance and triggering of an immune response (Figure 8). It was known before that brushite and HaP can induce the conversion of C3 ta C3b.[48] We found that both nonmodified brushite and HaP NPs activated the C3a complement, but the amount of activation was much less than the positive control (cobra venom factor). It was revealed that the concentration of the NPs did not have a noticeable effect on the activation of C3a complement. Also, it was shown the amine functionalization of the CaP NPs can slightly increase the amount of complement activation. This observation is in agreement with the arguments that $-NH_2$ functionalized surfaces can activate C3 complement because of either hydrophobic adsorption or covalent attachment of C4b complement to $-NH_2$ group.[49]

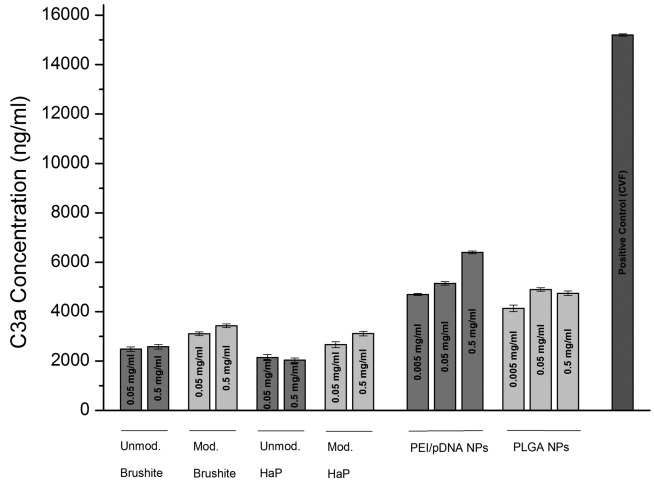

Figure 8. Results of C3a complement activation assay for unmodified and modified brushite and HaP NPs at different concentrations. PEI particles and PLGA particles serve as benchmark particulate references.

To have a better perspective, we compared the effect of CaP NPs on activation of C3 complement with two benchmark NPs used in drug/gene delivery (PEI/pDNA and PLGA NPs). It can be seen that CaP NPs can be safer in comparison to polymeric NPs regarding triggering the complement cascade.

DOI: 10.1021/am507193a
ACS Appl. Mater. Interfaces 2015, 7, 5124−5133

4. CONCLUSION

This paper provides an overview on the biological characteristics of novel amino-modified CaP NPs that were recently developed in our group. We showed that the aminosilane coating did not prevent the degradation of the particles and both types of amino-modified CaP NPs are completely degradable within several days. Brushite had a significantly faster degradation rate than HaP at neutral pH. This feature is useful for local, transient transfection, where the carrier does not need long time to reach the target and should have no chance to accumulate even upon repeated application.

It was shown that both particles were capable of transfecting two different cell lines. However, in all the transfection experiments, brushite NPs showed more favorable transfection results in comparison with HaP NPs. The cytotoxicity of the NPs was in unproblematic range in the concentrations of optimum transfection. The immune activation studies were promising as we observed only a mild triggering, comparable to the one of established NPs like PLGA. An interesting finding regarding this experiment was that the amine functionalization of the NPs rather reduced the immune activation. As a cumulative result, we managed to synthesize CaP NPs with enough positive surface charge to keep them dispersed in empty and in pDNA adsorbed state. Nevertheless, the positive surface charge was in tolerable range with regard to the cytotoxicity and immune activation studies. Comparing the two types of CaP NPs, although brushite NPs had a higher positive surface charge than HaP NPs, it showed more promising results in toxicity and cytokine release experiments. We conclude from these results, that at least in this set of in vitro studies the higher colloidal stability of brushite NPs is of higher impact than the slightly higher surface charge.

The results presented in this paper support our hypothesis about the capability of these novel types of CaP NPs to act as successful gene delivery vectors. Although this is a significant step forward regarding the use of CaP NPs in nonviral gene therapy, more investigations are needed to prove their in vivo efficiency.

■ ASSOCIATED CONTENT

Supporting Information

Gel retardation assay results for amino-modified brushite and HaP NPs to analyze pDNA condensation capacity, Ca^{2+} and Si^{4+} ions release diagrams related to degradation experiment (based on the absolute values), autocorrelation curves, hydrodynamic size, and PDI data obtained from DLS for the NPs incubated for different time periods and related concentration of the particles obtained by NTA method as supporting methods to monitor the particle disintegration and results of LDH toxicity assay. This material is available free of charge via the Internet at http://pubs.acs.org.

■ AUTHOR INFORMATION

Corresponding Authors

*E-mail: Claus-Michael.Lehr@helmholtz-hzi.de.
*E-mail: Brigitta.Loretz@helmholtz-hzi.de

Author Contributions

The manuscript was written through contributions of all authors. All authors have given approval to the final version of the manuscript.

Notes

The authors declare no competing financial interest.

■ ACKNOWLEDGMENTS

The authors cordially thank Dr. Ralf Kautenburger (Inorganic Solid State Chemistry, Saarland Uni.) for his help regarding ICP-OES experiments, Mr. Peter Meiers for his assistances regarding preparing the blood and Mr. Marijas Jurisic for his assistances regarding flow cytometry measurements. Furthermore, we like to thank Ms. Heike Stumpf, Ms. Petra König, and Ms. Sarina Hager (Department of Biopharm. & Pharm. Tech., Saarland Uni.) for their support regarding cell culture experiments. Ms. Nicole Kunschke and Ms. Hiroe Yamada were appreciated regarding the kind donation of polymeric benchmark NPs.

■ REFERENCES

(1) Ginn, S. L.; Alexander, I. E.; Edelstein, M. L.; Abedi, M. R.; Wixon, J. Gene Therapy Clinical Trials Worldwide to 2012 - an Update. *J. Gene Med.* **2013**, *15*, 65−77.

(2) Gaj, T.; Gersbach, C. A.; Barbas, C. F. ZFN, TALENS and CRISPR/CAS-Based Methods for Genome Engineering. *Trends Biotechnol.* **2013**, *31*, 397−405.

(3) Bedell, V. M.; Wang, Y.; Campbell, J. M.; Poshusta, T. L.; Starker, C. G.; Krug, R. G.; Tan, W. F.; Penheiter, S. G.; Ma, A. C.; Leung, A. Y. H.; Fahrenkrug, S. C.; Carlson, D. F.; Voytas, D. F.; Clark, K. J.; Essner, J. J.; Ekker, S. C. In Vivo Genome Editing Using a High-Efficiency TALEN System. *Nature* **2012**, *491*, 114−118.

(4) Atkinson, H.; Chalmers, R. Delivering the Goods: Viral and Non-Viral Gene Therapy Systems and the Inherent Limits on Cargo DNA and Internal Sequences. *Genetica* **2010**, *138*, 485−498.

(5) Chailertvanitkul, V. A.; Pouton, C. W. Adenovirus: A Blueprint for Non-Viral Gene Delivery. *Curr. Opin. Biotechnol.* **2010**, *21*, 627−632.

(6) Cheng, Y. *Dendrimer-Based Drug Delivery Systems: From Theory to Practice*; John Wiley & Sons: Hoboken, NJ, 2012.

(7) Elzoghby, A. O.; Samy, W. M.; Elgindy, N. A. Protein-Based Nanocarriers as Promising Drug and Gene Delivery Systems. *J. Controlled Release* **2012**, *161*, 38−49.

(8) Yin, L. C.; Song, Z. Y.; Kim, K. H.; Zheng, N.; Tang, H. Y.; Lu, H.; Gabrielson, N.; Cheng, J. J. Reconfiguring the Architectures of Cationic Helical Polypeptides to Control Non-Viral Gene Delivery. *Biomaterials* **2013**, *34*, 2340−2349.

(9) Zhi, D. F.; Zhang, S. B.; Wang, B.; Zhao, Y. N.; Yang, B. L.; Yu, S. J. Transfection Efficiency of Cationic Lipids with Different Hydrophobic Domains in Gene Delivery. *Bioconjugate Chem.* **2010**, *21*, 563−577.

(10) Khan, W.; Hosseinkhani, H.; Ickowicz, D.; Hong, P. D.; Yu, D. S.; Domb, A. J. Polysaccharide Gene Transfection Agents. *Acta Biomater.* **2012**, *8*, 4224−4232.

(11) Sun, X. L.; Zhang, N. Cationic Polymer Optimization for Efficient Gene Delivery. *Mini-Rev. Med. Chem.* **2010**, *10*, 108−125.

(12) Dandekar, P.; Jain, R.; Keil, M.; Loretz, B.; Muijs, L.; Schneider, M.; Auerbach, D.; Jung, G.; Lehr, C. M.; Wenz, G. Cellular Delivery of Polynucleotides by Cationic Cyclodextrin Polyrotaxanes. *J. Controlled Release* **2012**, *164*, 387−393.

(13) Yamada, H.; Loretz, B.; Lehr, C. M. Design of Starch-Graft-PEI Polymers: An Effective and Biodegradable Gene Delivery Platform. *Biomacromolecules* **2014**, *15*, 1753−1761.

(14) Nafee, N.; Taetz, S.; Schneider, M.; Schaefer, U. F.; Lehr, C. M. Chitosan-Coated PLGA Nanoparticles for DNA/RNA Delivery: Effect of the Formulation Parameters on Complexation and Transfection of Antisense Oligonucleotides. *Nanomedicine* **2007**, *3*, 173−183.

(15) Pissuwan, D.; Niidome, T.; Cortie, M. B. The Forthcoming Applications of Gold Nanoparticles in Drug and Gene Delivery Systems. *J. Controlled Release* **2011**, *149*, 65−71.

(16) Jiang, S.; Eltoukhy, A. A.; Love, K. T.; Langer, R.; Anderson, D. G.; Lipidoid-Coated Iron, Oxide Nanoparticles for Efficient DNA and siRNA Delivery. *Nano Lett.* **2013**, *13*, 1059−1064.

DOI: 10.1021/am507193a
ACS Appl. Mater. Interfaces 2015, 7, 5124−5133

(17) Csogor, Z.; Nacken, M.; Sameti, M.; Lehr, C. M.; Schmidt, H. Modified Silica Particles for Gene Delivery. *Mater. Sci. Eng., C* **2003**, *23*, 93−97.
(18) Bhakta, G.; Sharma, R. K.; Gupta, N.; Cool, S.; Nurcombe, V.; Maitra, A. Multifunctional Silica Nanoparticles with Potentials of Imaging and Gene Delivery. *Nanomedicine* **2011**, *7*, 472−479.
(19) Kumar, M. N. V. R.; Sameti, M.; Mohapatra, S. S.; Kong, X.; Lockey, R. F.; Bakowsky, U.; Lindenblatt, G.; Schmidt, H.; Lehr, C. M. Cationic Silica Nanoparticles as Gene Carriers: Synthesis, Characterization and Transfection Efficiency in Vitro and in Vivo. *J. Nanosci. Nanotechnol.* **2004**, *4*, 876−881.
(20) Li, S. D.; Li, J. H.; Wang, C. J.; Wang, Q.; Cader, M. Z.; Lu, J.; Evans, D. G.; Duan, X.; O'Hare, D. Cellular Uptake and Gene Delivery Using Layered Double Hydroxide Nanoparticles. *J. Mater. Chem. B* **2013**, *1*, 61−68.
(21) Kim, M. H.; Na, H. K.; Kim, Y. K.; Ryoo, S. R.; Cho, H. S.; Lee, K. E.; Jeon, H.; Ryoo, R.; Min, D. H. Facile Synthesis of Monodispersed Mesoporous Silica Nanoparticles with Ultralarge Pores and Their Application in Gene Delivery. *ACS Nano* **2011**, *5*, 3568−3576.
(22) Nouri, A.; Castro, R.; Santos, J. L.; Fernandes, C.; Rodrigues, J.; Tomas, H. Calcium Phosphate-Mediated Gene Delivery Using Simulated Body Fluid (SBF). *Int. J. Pharm.* **2012**, *434*, 199−208.
(23) Oyane, A.; Wang, X. P.; Sogo, Y.; Ito, A.; Tsurushima, H. Calcium Phosphate Composite Layers for Surface-Mediated Gene Transfer. *Acta Biomater.* **2012**, *8*, 2034−2046.
(24) Lee, K.; Oh, M. H.; Lee, M. S.; Nam, Y. S.; Park, T. G.; Jeong, J. H. Stabilized Calcium Phosphate Nano-Aggregates Using a Dopa-Chitosan Conjugate for Gene Delivery. *Int. J. Pharm.* **2013**, *445*, 196−202.
(25) Wang, K. W.; Zhou, L. Z.; Sun, Y.; Wu, G. J.; Gu, H. C.; Duan, Y. R.; Chen, F.; Zhu, Y. J. Calcium Phosphate/PLGA-mPEG Hybrid Porous Nanospheres: A Promising Vector with Ultrahigh Gene Loading and Transfection Efficiency. *J. Mater. Chem.* **2010**, *20*, 1161−1166.
(26) Li, J.; Chen, Y. C.; Tseng, Y. C.; Mozumdar, S.; Huang, L. Biodegradable Calcium Phosphate Nanoparticle with Lipid Coating for Systemic Sirna Delivery. *J. Controlled Release* **2010**, *142*, 416−421.
(27) Sokolova, V.; Knuschke, T.; Buer, J.; Westendorf, A. M.; Epple, M. Quantitative Determination of the Composition of Multi-Shell Calcium Phosphate-Oligonucleotide Nanoparticles and Their Application for the Activation of Dendritic Cells. *Acta Biomater.* **2011**, *7*, 4029−4036.
(28) Pittella, F.; Cabral, H.; Maeda, Y.; Mi, P.; Watanabe, S.; Takemoto, H.; Kim, H. J.; Nishiyama, N.; Miyata, K.; Kataoka, K. Systemic siRNA Delivery to a Spontaneous Pancreatic Tumor Model in Transgenic Mice by Pegylated Calcium Phosphate Hybrid Micelles. *J. Controlled Release* **2014**, *178*, 18−24.
(29) Mostaghaci, B.; Loretz, B.; Haberkorn, R.; Kickelbick, G.; Lehr, C. M. One-Step Synthesis of Nanosized and Stable Amino-Functionalized Calcium Phosphate Particles for DNA Transfection. *Chem. Mater.* **2013**, *25*, 3667−3674.
(30) Boussif, O.; Lezoualch, F.; Zanta, M. A.; Mergny, M. D.; Scherman, D.; Demeneix, B.; Behr, J. P. A Versatile Vector for Gene and Oligonucleotide Transfer into Cells in Culture and in-Vivo - Polyethylenimine. *Proc. Natl. Acad. Sci. U.S.A.* **1995**, *92*, 7297−7301.
(31) Kumar, M. N. V. R.; Bakowsky, U.; Lehr, C. M. Preparation and Characterization of Cationic PLGA Nanospheres as DNA Carriers. *Biomaterials* **2004**, *25*, 1771−1777.
(32) Lane, D.; Prentki, P.; Chandler, M. Use of Gel Retardation to Analyze Protein-Nucleic Acid Interactions. *Microbiol. Rev.* **1992**, *56*, 509−528.
(33) Kunzmann, A.; Andersson, B.; Thurnherr, T.; Krug, H.; Scheynius, A.; Fadeel, B. Toxicology of Engineered Nanomaterials: Focus on Biocompatibility, Biodistribution and Biodegradation. *Biochim. Biophys. Acta, Gen. Subj.* **2011**, *1810*, 361−373.
(34) Epple, M.; Kovtun, A. Functionalized Calcium Phosphate Nanoparticles for Biomedical Application. *Key Eng. Mater.* **2010**, *441*, 299−305.
(35) Kalita, S. J.; Bhardwaj, A.; Bhatt, H. A. Nanocrystalline Calcium Phosphate Ceramics in Biomedical Engineering. *Mater. Sci. Eng., C* **2007**, *27*, 441−449.
(36) Olmos, D.; Gonzalez-Benito, J.; Aznar, A. J.; Baselga, J. Hydrolytic Damage Study of the Silane Coupling Region in Coated Silica Microfibres: pH and Coating Type Effects. *J. Mater. Process. Technol.* **2003**, *143*, 82−86.
(37) Asenath-Smith, E.; Chen, W. How to Prevent the Loss of Surface Functionality Derived from Aminosilanes. *Langmuir* **2008**, *24*, 12405−12409.
(38) Zhou, J. B.; Liu, J.; Cheng, C. J.; Patel, T. R.; Weller, C. E.; Piepmeier, J. M.; Jiang, Z. Z.; Saltzman, W. M. Biodegradable Poly(Amine-co-Ester) Terpolymers for Targeted Gene Delivery. *Nat. Mater.* **2012**, *11*, 82−90.
(39) Akuta, K.; Abe, M.; Kondo, M.; Yoshikawa, T.; Tanaka, Y.; Yoshida, M.; Miura, T.; Nakao, N.; Onoyama, Y.; Yamada, T.; Mukoujima, T.; Tsukada, K. Combined Effects of Hepatic Arterial Embolization Using Degradable Starch Microspheres (DSM) in Hyperthermia for Liver-Cancer. *Int. J. Hyperthermia* **1991**, *7*, 231−242.
(40) Li, S.; Wang, Y.; Zhang, J.; Yang, W. H.; Dai, Z. H.; Zhu, W.; Yu, X. Q. Biodegradable Cross-Linked Poly(Amino Alcohol Esters) Based on LMW PEI for Gene Delivery. *Mol. Biosyst.* **2011**, *7*, 1254−1262.
(41) Yu, T.; Malugin, A.; Ghandehari, H. Impact of Silica Nanoparticle Design on Cellular Toxicity and Hemolytic Activity. *ACS Nano* **2011**, *5*, 5717−5728.
(42) Fischer, D.; Li, Y. X.; Ahlemeyer, B.; Krieglstein, J.; Kissel, T. In Vitro Cytotoxicity Testing of Polycations: Influence of Polymer Structure on Cell Viability and Hemolysis. *Biomaterials* **2003**, *24*, 1121−1131.
(43) Singh, S. K.; Singh, M. K.; Kulkarni, P. P.; Sonkar, V. K.; Gracio, J. J. A.; Dash, D. Amine-Modified Graphene. Thrombo-Protective Safer Alternative to Graphene Oxide for Biomedical Applications. *ACS Nano* **2012**, *6*, 2731−2740.
(44) Shute, J. Interleukin-8 Is a Potent Eosinophil Chemoattractant. *Clin. Exp. Allergy* **1994**, *24*, 203−206.
(45) Lucia, P.; Cinzia, C.; Roberta, D. B.; Michele, G.; Umberto, M.; Cucchiarini, L.; Nappo, G.; Alloni, R.; Coppola, R.; Dugo, L.; Dacha, M. Effects of Reactive Oxygen Species on Mitochondrial Content and Integrity of Human Anastomotic Colorectal Dehiscence: A Preliminary DNA Study. *Can. J. Gastroenterol.* **2011**, *25*, 433−439.
(46) Thevenot, P.; Hu, W.; Tang, L. Surface Chemistry Influences Implant Biocompatibility. *Curr. Top. Med. Chem.* **2008**, *8*, 270−80.
(47) Pissuwan, D.; Kumagai, Y.; Smith, N. I. Effect of Surface-Modified Gold Nanorods on the Inflammatory Cytokine Response in Macrophage Cells. *Part. Part. Syst. Charact.* **2013**, *30*, 427−433.
(48) Klein, C. P.; de Groot, K.; van Kamp, G. Activation of Complement C3 by Different Calcium Phosphate Powders. *Biomaterials* **1983**, *4*, 181−4.
(49) Pondman, K. M.; Sobik, M.; Nayak, A.; Tsolaki, A. G.; Jakel, A.; Flahaut, E.; Hampel, S.; Ten Haken, B.; Sim, R. B.; Kishore, U. Complement Activation by Carbon Nanotubes and Its Influence on the Phagocytosis and Cytokine Response by Macrophages. *Nanomedicine* **2014**, *10*, 1287−1299.

DOI: 10.1021/am507193a
ACS Appl. Mater. Interfaces 2015, 7, 5124−5133